Conference on Modelling Fluid Flow (CMFF'22)
The 18th International Conference on Fluid Flow Technologies
Budapest, Hungary, August 30 -September 2, 2022

SURFACE LAYER'S SOUND SPEED PROFILES: CLIMATOLOGICAL ANALYSIS AND APPLICATION FOR THE CNOSSOS-EU NOISE MODEL

Tamás WEIDINGER[1], Petra FRITZ[2], Arun GANDHI[2], Abderrahmane MENDYL[2], Ágoston Vilmos TORDAI[2]

[1] Corresponding Author, Department of Meteorology, Institute of Geography and Earth Sciences, Faculty of Sciences, Eötvös Loránd University, Pázmány Péter sétány 1/A, H-1117 Budapest, Hungary. Tel.: +36 1 372 2545, E-mail: weidi@staff.elte.hu
[2] Department of Meteorology, Institute of Geography and Earth Sciences, Faculty of Sciences, Eötvös Loránd University. E-mail: fritzpetra31@gmail.com, arun.elte@gmail.com, mendyl.abderrahmane@gmail.com, tordaiagoston@gmail.com

ABSTRACT

Investigation and regulation of noise pollution and exposure are important environmental tasks, which require micrometeorological knowledge. The harmonised CNOSSOS-EU noise model requires detailed meteorological databases to determine noise propagation between the source and receptor points. For this reason, it is necessary to determine the relative frequencies of sound speed profiles based on wind speed, direction, and stability conditions for different source-receptor directions and for different times of the day (nighttime, daytime, and evening).

Meteorological variables are commonly used in noise modelling (optimally at least 5-year long, hourly dataset); wind speed and direction, temperature, humidity, and atmospheric stability. If the surface turbulence parameters are available, the atmospheric stability can be calculated directly. The noise propagation conditions according to the standardized procedures (stability classes 25 or 2) are calculated based on the SYNOP stations data from Hungarian Meteorological Service (HMS) and the ERA5 meteorological reanalysis database.

Our main goal was to determine the frequency distribution of stability classes for different source-receiver directions with various levels of aggregation using 25 or 2 stability classes. We also estimated the uncertainties of the stability classes favourable (homogeneous) and unfavourable (downward-refraction) in the developed preprocessor.

Keywords: CNOSSOS-EU, noise model, ERA5, meteorological preprocessor, sound speed profiles, stability classes, turbulence

Nomenclature

L_*	$[m]$	Monin-Obukhov length
L_{LT}	$[dB]$	long-term average sound levels
L_H	$[dB]$	homogenous conditions
L_F	$[dB]$	downward-refraction conditions
R_d	$[J/kg\ K]$	specific gas constant for dry air
T_*	$[K]$	temperature scale
T_v	$[K]$	virtual temperature
T_{v0}	$[K]$	reference virtual temperature near the surface
V	$[m/s]$	wind speed
a	$[m/s]$	constant of logarithmic term in the sound speed profile
a_c	$[m/s]$	in virtual temperature profile
a_u	$[m/s]$	in wind speed profile
b	$[1/m]$	constant of the linear term in sound speed profile
b_c	$[1/m]$	in virtual temperature profile
b_u	$[1/m]$	in wind speed profile
c	$[m/s]$	speed of sound in the atmosphere
c_0	$[m/s]$	speed of sound near the surface
c_{ad}	$[m/s]$	adiabatic sound speed
c_{pd}	$[J/kg\ K]$	specific heat capacity for dry air with constant pressure
c_{vd}	$[J/kg\ K]$	specific heat capacity for dry air with constant volume
e	$[Pa]$	water vapour pressure
k	[-]	ratio of c_{pd} and c_{vd}
p	$[Pa]$	pressure
p_f	[-]	probability of occurrence of downward-refraction conditions in the long term (min. 1 year)
q	$[kg/kg]$	specific humidity
u	$[m/s]$	wind speed in source-receptor direction
z	$[m]$	height above the surface
z_0	$[m]$	roughness length
α	[°]	wind direction
β	[°]	position of the source point
γ_d	$[°C/m]$	dry adiabatic temperature gradient $\gamma_d = 0.00976\ °C/m$
φ	[°]	angle between the direction of the sound propagation and the wind
κ	[-]	von Kármán constant

1. INTRODUCTION

Investigation of atmospheric sound propagation is practically important because noise pollution load from transport, industrial production, and also from entertainment and concerts are significant. In sound propagation modelling, there are different types of point, line, and areal sources [1, 2]. We concentrate only on the point sources. Sound levels between 30-90 *dB* are the most common in everyday life, and they are especially bothersome at night. Environmental standards specify the various noise pollution limits in detail. In Hungary, the outdoor sound propagation (MSZ 15036) standard provides a general methodology for noise propagation calculation [3, 4]. „The departmental order 93/2007 (XII. 18.) on the noise emission standards determination" defines the noise limit values for various residential, transport, industrial, and other activities [5]. The average daily noise exposure of industrial buildings during daytime is 56 *dB* and 50 *dB* at nighttime respectively in Hungary. The average noise exposure for traffic sources is 73 *dB* on a daily scale and 65 *dB* at night, respectively. Hospitals, health, and educational institutes are a priority; the optimal noise exposure should be less than 35 *dB*.

Approximately 20% of the European population is subject to long-term excessive noise exposure which is harmful to their health [6]. According to the World Health Organisation (WHO), noise is the second most common environmental cause of health problems, just after the particle matters (PM). Around 30-35% of Budapest's population live in noisy conditions hazardous to their health. The difference between nighttime and daytime noise level is only 4-7 *dB* on average, which means that even at night the noise exposure is significant.

The European Union agreed to harmonise noise propagation modelling and production of noise maps in 2015 [7]. The developed CNOSSOS-EU noise model requires a detailed meteorological database for the calculation of the sound speed profiles between the source and the receptor point [8-10]. The task is to determine the relative frequency of these homogeneous (decreasing or constant with height) and downward-refraction (increasing with height) sound speed profiles in terms of noise exposure. The calculations are provided based on the hourly measurements of temperature, atmospheric stability, wind speed, and direction at different times of the day and source-receiver directions using 5-10 years of time series.

After an overview of the theoretical background of noise propagation, the role of the different atmospheric stability classes is described. Calculation of the Pasquill-Gifford stability classes and the generation of near-surface sound speed profiles are also presented based on the calculation of wind speed and virtual temperature profiles using the Monin-Obukhov similarity theory. Based on the methodology, firstly 25 types of stability and wind speed dependent sound speed profiles were used [8].

The Hungarian meteorological preprocessor developed for the CNOSSOS-EU noise propagation model is also provided. The probability of occurrence of downward-refraction conditions (p_f) is presented based on ten years of hourly SYNOP observations from the György Marczell Main Observatory of the HMS (Budapest, 12843). Three parts of the day are investigated separately: night (22-06 *h* local time), day (06-18 *h*) and evening (18-22 *h*). Differences among years are also analysed. Results obtained from five additional weather stations with a 5-year long time series are also presented. Finally, the comparison of results (p_f) from the measured and the ERA5 reanalysis dataset [11] for Budapest was provided. The ERA5 reanalysis database – together with the meteorological variables – contains the radiation balance components (short- and longwave) and the surface energy budget components, such as momentum, sensible and latent heat fluxes, friction velocity (u_*), temperature scale (T_*), and Monin–Obukhov length (L_*) [12, 13]. The occurrence of downward-refraction conditions (p_f) is calculated based on the meteorological variables and directly from the surface layer turbulence characteristics.

2. SOUND SPEED PROPAGATION

Sound waves are density waves. The equation of propagation velocity (c) in moist air with pressure p, temperature, T and water vapour pressure e is:

$$c_{ad} = \sqrt{k \cdot R_d \cdot T_v}$$

where $k = c_{pd} / c_{vd} = 7/5 = 1.4$ is the ratio of the specific heat capacity for dry air at constant pressure and constant volume, $R_d = 287\, J/kg\, K$. T_v, is the virtual temperature.

$$T_v = T(1 + 0.608 \cdot q)$$

where the specific humidity is the ratio of the water vapour density and the wet air density [13]:

$$q = 0.622 \frac{e}{p - 0.378 \cdot e}$$

If the sound travels from a „more acoustically dense" medium with a lower propagation speed (e.g., a lower temperature) to a „less acoustically dense" medium, it will be diffracted (Figure 1a, b). The propagation speed of the wave increases as it enters the acoustically less dense medium. The direction of sound propagation and the angle of refraction of the sound wave at the boundary of the two media (the angle subtended by the normal of the surface) are also changed. The ratio of the sine of the two angles is equal to the ratio of the speed of sound in the two

media. This is the well-known Snellius-Descartes law, in wave theory [14].

The speed of sound decreases with the height during the daytime and increases at the night (inversion) due to the stratification (Figure 1a, b).

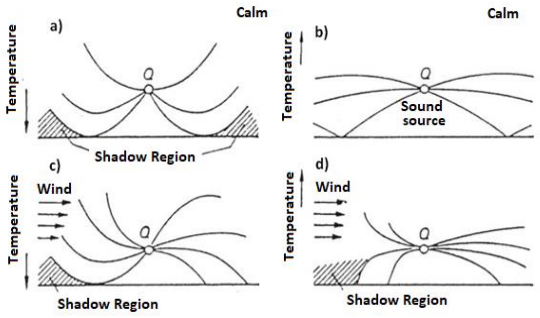

Figure 1: Sound propagation (along curved paths due to diffraction) as a function of temperature stratification during calm periods for unstable (a) and stable (b) stratification, with wind profile modification (c, d) [13].

The noise propagation is modified by the relative wind speed (upwind, crosswind, and downwind depending on the source-receiver position) in the direction of the source-receiver points. Downwind is blowing from the noise source to the receptor point in the direction of the sound propagation and increasing it (Figure 1c, d). Note that the total crosswind (the wind vector perpendicular to the line of the source-receiver points) has no effect on the sound propagation.

Thus, the speed of sound propagation depends on i) the wind speed profile ($u(z)$) and the direction of sound propagation, ii) the angle φ between the point source and the wind flag (Figure 2), as seen from the receptor point in the „centre of the circle", and iii) the temperature changes with height. In a full downwind, the wind blows from the noise source to the receptor point. The angle between the actual wind direction (the wind flag) and the noise source is then $\varphi = 0°$, while $\varphi = 180°$ for upwind and $\varphi = 90°$ or $\varphi = 270°$ for full crosswinds. (In meteorology, the current wind direction is the direction from which the wind blows always on horizontal plane.) The wind develops or strengthens the shadow zone on the upstream side (wind blowing from the receptor point towards the sound source); while on the downstream side, the wind weakens or dissipates the shadow zone, increasing the noise exposure. Note that wind speed always increases with height in the surface layer. For indifferent stratification, we use a logarithmic profile approximation. In the case of unstable stratification, the wind speed increases less than logarithmically with height, while in stable stratification it increases more than logarithmically.

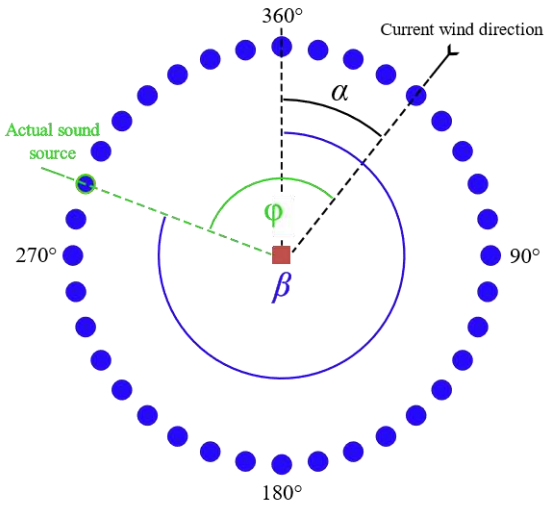

Figure 2: Source-receptor relationships. For a given wind direction (α), the hypothetical noise sources are positioned at every 10 degrees and the angle φ is subtended by the „wind flag" (actual wind direction) as seen from the receptor point. The hypothetical noise sources are indicated by the blue circles and the receptor point by the red rectangle. β corresponds to the position of the actual sound source. Propagation categories (homogeneous or downward-refraction) are given for the 36 hypothetical sources in each hour. This is a typical crosswind situation between the actual sound source (green) and the receiver point (red).

2.1. Sound speed profiles

The variation of the sound speed with height depends on the wind speed and virtual temperature profiles and the angle between the current noise source and the wind direction (Figure 2). Log-linear profile approximations were used for stable and unstable stratifications with different constants, obtained by integrating the simplified universal functions of the Monin-Obukhov similarity theory [12, 16]. The shapes of the commonly used sound speed profiles are in [8, 9, 10, 15]:

$$c(z) = c_{ad}(z) + u(z) = \\ = a \cdot \ln\left(1 + \frac{z}{z_0}\right) + b \cdot z + c_0$$

$$c_{ad}(z) \approx c_0 + \frac{1}{2}\frac{k \cdot R_d}{c_0}\left(T_v(z) - T_{v_0}\right) \approx \\ \approx c_0 + a_c \cdot \ln\left(1 + \frac{z}{z_0}\right) + b_c z$$

$$u(z) = V(z) \cdot \cos\varphi \approx +a_u \cdot \ln\left(1 + \frac{z}{z_0}\right) + b_u z$$

with $a = a_u + a_c$, $b = b_u + b_c$.

The constants in the equations are defined as a function of the atmospheric stability using the

Pasquill-Gifford stability categories [17], following the methodology [8, 9, 10]. We use 5 stability classes based on time of day and cloud cover data (Table 1). There are also more complex methodologies [17], but our purpose is to build up a standard methodology that is simple and easy to use. Daytime hours are defined as the estimated global irradiance from cloud cover above 20 W/m^2.

Table 1: Stability classes, S1 to S5, from unstable to stable.

Stability class	day/night, cloud cover (octas)
S1	day, 0 - 2
S2	day, 3 - 5
S3	day, 6 - 8
S4	night, 5 - 8
S5	night, 0 - 4

The effect of the wind profile on sound propagation depends on the source-receptor line and the angle φ subtended by the wind direction. The crosswind does not affect the sound propagation ($\cos\varphi = 0$). The simplified universal functions used for the calculations [8] were constructed based on [20]. The shape of the logarithmic term:

$$a_u = \frac{u_* \cdot \cos\varphi}{\kappa}$$

The linear term gives the deviation from the logarithmic profile. In the daytime, for unstable stratification ($T_* < 0$, $L_* < 0$, Table 2-5):

$$b_u = \frac{u_* \cdot \cos\varphi}{\kappa} \cdot \frac{1}{L_*}$$

At nighttime, with stable stratification ($T_* > 0$, $L_* > 0$, Table 2–5):

$$b_u = \frac{u_* \cdot \cos\varphi}{\kappa} \cdot \frac{4.7}{L_*}$$

Similar principles are used for the constants of the virtual temperature profile in unstable and stable stratifications:

$$a_c \approx \frac{1}{2}\frac{k \cdot R_d}{c_0} \cdot 0.74\frac{T_*}{\kappa}$$

$$b_c \approx \frac{1}{2}\frac{k \cdot R_d}{c_0} \cdot \left(\frac{T_*}{\kappa}\frac{0.74}{L_*} + \gamma_d\right) \text{ during day}$$

$$b_c \approx \frac{1}{2}\frac{k \cdot R_d}{c_0} \cdot \left(\frac{T_*}{\kappa}\frac{4.7}{L_*} + \gamma_d\right) \text{ during night}$$

Table 2: Wind speed classes W1 to W5 according to wind speeds at 10 m above the ground and estimated friction velocity (u_*).

Wind speed class	$V(z = 10\ m)$	u_*
W1	0 - 1 *m/s*	0.00 *m/s*
W2	1 - 3 *m/s*	+0.13 *m/s*
W3	3 - 6 *m/s*	+0.30 *m/s*
W4	6 - 10 *m/s*	+0.53 *m/s*
W5	>10 *m/s*	+0.87 *m/s*

Table 3: Temperature scale (T_*, $°C$) in different wind speed (W1-W5) and stability classes (S1–S5) classes.

	S1	S2	S3	S4	S5
W1	−0.4	−0.2	0	+0.2	0.3
W2	−0.2	−0.1	0	+0.1	0.2
W3	−0.1	−0.05	0	+0.05	0.1
W4	−0.05	0	0	0	0.05
W5	0	0	0	0	0

Table 4: Values of $1/L_*$ ($1/m$) for different wind speed and stability classes.

	S1	S2	S3	S4	S5
W1	−0.08	−0.05	0	+0.04	+0.06
W2	−0.05	−0.02	0	+0.02	+0.04
W3	−0.02	−0.01	0	+0.01	+0.02
W4	−0.01	0	0	0	+0.01
W5	0	0	0	0	0

Table 5: The effect of the angle between the sound propagation direction and the wind on sound speed profile calculation.

		$u_* \cdot \cos\varphi$
V1= –W5	upwind $V \cdot cos\varphi < -1\ m/s$	–0.87 m/s
V2= –W4		–0.53
V3= –W3		–0.30
V4= –W2		–0.13
V5= ±W1	crosswind	±0.00 m/s
V6= +W2	downwind $V \cdot cos\varphi > 1\ m/s$	+0.13
V7= +W3		+0.30
V8= +W4		+0.53
V9= +W5		+0.87 m/s

2.2. Sound propagation modelling

For us as data providers, it is important to provide the probability of occurrence of downward-refraction (p_f) and homogeneous ($1 - p_f$) conditions for sound propagation, for the calculation of the noise exposure from a given direction to a fixed receptor point (Figure 2).

The variation of sound speed with height by the derivation of the profile equation is:

$$\frac{\partial c}{\partial z} = \frac{a}{z + z_0} + b$$

where the height above the surface is $z = 4\ m$ and the roughness length is $z_0 = 0.1\ m$. We distinguished between favourable cases

(homogeneous conditions) $\frac{\partial c}{\partial z} \leq 0$ and unfavourable cases (downward-refraction) $\frac{\partial c}{\partial z} > 0$ in terms of noise exposure.

The hypothetical noise sources were positioned at 10 degrees around the receptor point (Figure 2) according to the wind directions given in the SYNOP reports. The profile type is provided for each of the 36 cases based on the current a and b values (5-5 classes). The 25 possible classes are given in Tables 6 and 7.

Table 6: Values of a in different classes (a_1, a_5) based on categories of Table 3-5.

Interval	Discrete value (m/s)
$-\infty < a \leq -0.7$	$a_1 = -1.0$
$-0.7 < a \leq -0.2$	$a_2 = -0.4$
$-0.2 < a \leq +0.2$	$a_3 = 0$
$+0.2 < a \leq +0.7$	$a_4 = +0.4$
$+0.7 < a \leq +\infty$	$a_5 = +1.0$

Table 7: Values of b in different classes (b_1, b_5) based on categories of Table 3-5.

Interval	Discrete value ($1/m$)
$-\infty < b \leq -0.08$	$b_1 = -0.12$
$-0.08 < b \leq -0.02$	$b_2 = -0.04$
$-0.02 < b \leq +0.02$	$b_3 = 0$
$+0.02 < b \leq +0.08$	$b_4 = +0.04$
$+0.08 < b \leq +\infty$	$b_5 = +0.12$

The long-term average noise level (L_{LT}) is calculated as the logarithmic sum of the sound pressure levels in decibel (dB) on a logarithmic scale, weighted by the occurrence rate of sound pressure levels between the meteorological conditions L_F, which are „unfavourable" for noise propagation (downward-refraction), and L_H, which are „favourable" for noise propagation (homogeneous cases):

$$L_{LT} = 10 \times \lg\left(p_f \cdot 10^{\frac{L_F}{10}} + \left(1 - p_f\right) \cdot 10^{\frac{L_H}{10}}\right)$$

where p_f is the ratio of the occurrence of downward-refraction conditions during the year, at three time periods of the day in local time (UTC + 1 and UTC + 2 in Central European Winter and Summer Time respectively): 06-18 h (daytime), 18-22 h (evening) and 22-06 h (nighttime), according to our rhythm of life and traffic dynamics.

In the previous standard noise propagation methods, the effect of the near-surface air layer was not taken into account with such detail [3, 4].

3. DATASET

The hourly synoptic datasets of HMS were downloaded from the Meteomanz and Ogimet websites for those years when cloud measurements were available. The amount of cloud cover is given in octaves (0, 1, ..., 8), the eighths of the sky. (Note that, from recent years most stations no longer have cloud detection.)

Hourly observations in Budapest (12843) for the 10-year period of 2009-2018 are analysed. We are also using out the data from five additional synoptic stations for 2014-2018, to get an idea of the differences of p_f, probability of occurrence of downward-refraction conditions within the country. These examined measurement sites are: Siófok, Pécs, Kecskemét, Szeged and Miskolc. The applicability of gridded datasets (here ERA5) is analysed at the closest grid cell to the Pestszentlőrinc, (12843) HMS station for the year-2014.

The quality control of the downloaded SYNOP databases was accomplished by filling in missing data. In cases of short data gaps (up to 6 measurement cycles missing), linear regression was used, while for longer data gaps, the gap-filling was performed based on the data of the previous and the following 1-3 days, leaving a maximum of 3 hours of adjustment time to fit the measured and interpolated data.

4. RESULTS

First of all, we looked at the 10-year data series for Budapest. In ~34% of cases, the daytime – between 06-18 h – was the most unfavourable (downward-refraction) period for noise propagation. In the evening, it is mostly stable between 18-22 *hrs*, and at night, between 22-06 *hrs* ~59% and ~64% respectively. There is a surprisingly high number of indifferent ($a = 0$, $b = 0$) sound velocity profiles, ranging from 15-35% depending on the time of day and receptor point orientation. Based on the results a recommendation can be made to introduce a third quasi-indifferent profile category into the meteorological preprocessor.

Next, we analysed the relative frequencies of the 25 stability categories ($a_1 - a_5$, $b_1 - b_5$). Out of the 25 possible classes, only 10 have an occurrence rate (Figure 3). This is understandable since, e.g., at high wind speeds, highly unstable stratification cannot develop. In this case, stratification is close to indifferent. During the daytime, we are more likely to see homogeneous sound propagation, while during the evening and nighttime, the speed of sound increases with height in most cases (downward-refraction). If we look at the differences between years, e.g., for indifferent cases, ($a = 0$, $b = 0$), the relative standard deviation (% of standard deviation/expected value) is around 5% in all three periods of the day. These are small values. Large

relative standard deviations (>15–20%) are usually found in cases of strong upwind and downwind situations, but the number of cases is small. In weak upwind and downwind situations (with high case rates), the standard deviations are between 10-20%. (These are crosswind situations).

The variation of the sound speed with height ($\partial c/\partial z$) was calculated at $z = 4\,m$ height after consultation with the experts of the Institute for Transport Sciences Non-profit Ltd. (KTI in Hungary). Considering i) the downward-refraction ($100 \cdot p_f$, %), ii) the homogeneous conditions ($(100 \cdot (1-p_f)$, %) and iii) the frequency of indifferent ($a = 0,\ b = 0$) situations which we classify as a subcategory within the homogeneous conditions group in the case of the two-category classification (Figure 4). The highest number of downward-refraction situations (potentially high noise exposure) is found in the northwest/northeast sector. This is understandable because this is the most common wind direction. The highest number of favourable (homogeneous) cases in terms of noise exposure is found on the opposite side. (Our „wind rose" in Figure 4. shows the frequency of cases (in %) depending on the location of the 36 virtual noise sources.) The probability of indifferent cases is high. During daytime hours, the values perpendicular to the main wind direction, together with light crosswind situations, exceed 35%. As expected, the asymmetric distribution of homogeneous and downward-refraction situations is clearly visible. In the evening and nighttime, the difference between the frequencies of each direction is smaller than during the daytime.

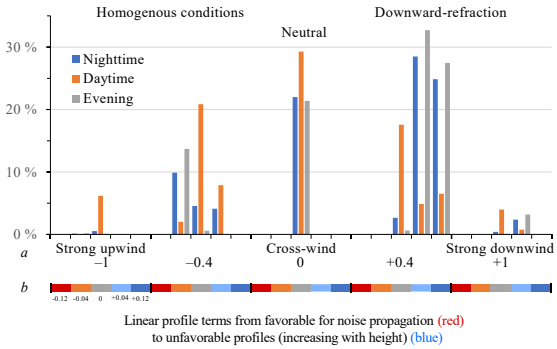

Figure 3: Relative frequency (%) of noise propagation in the 25 stability classes based on the hourly dataset (from 2009 to 2018) for Budapest (12843). Increasing values of *a* (logarithmic term) indicate increased wind speed in the direction of sound propagation while increasing values *b* (linear term) indicate stability (from unstable to stable stratification) and the current wind profile.

The standard deviations of the annual frequencies for each direction are small, between 1-5%, based on the 10-year Budapest data series.

Finally, we examined the differences between the highest and lowest annual relative frequencies (%) in each direction for the homogeneous and downward-refraction situations. The results for daytime hours are presented in Figure 5. The most significant differences are around 15% in the sectors that are perpendicular to the main wind direction. The smallest absolute deviations are in the north and south directions, with values of around 5%.

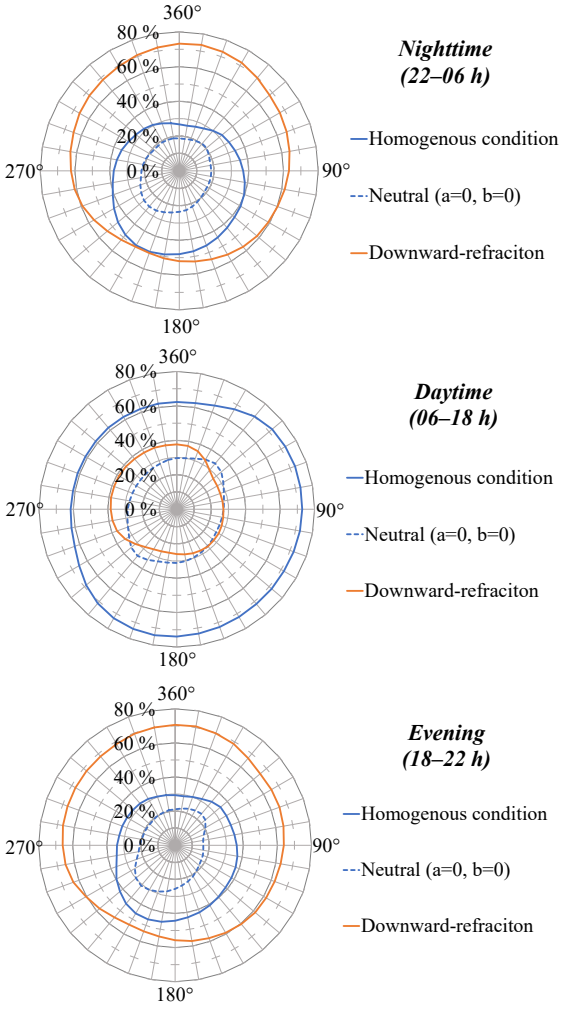

Figure 4: Noise pollution for homogeneous condition, downward-refraction cases, and indifferent stratification (a subcategory of homogenous condition) for nighttime, daytime, and evening in local time (Budapest, 2009-2018).

In addition to the 10-year Budapest dataset, we also analysed the average relative frequencies of probability p_f in all three time periods based on hourly data from 5 other SYNOP stations in Hungary for years between 2014 and 2018 (Figure 6). The difference between p_f values is less than 2% for the two 5-year periods in Budapest for each time period of the day. The variance within the two 5-year periods is less than 1% in the daytime, but not more

than 2% in the other two periods. Thus, it is sufficient to work with 5-year data series.

The results from Budapest and the five rural cities (except Miskolc) provide similar characteristics. The 5-year averages show differences of a few per cent (<5%). However, the evening and night p_f values for Miskolc are significantly higher than those of the other stations, by more than 20%. This is because of many unfavourable cases. The station is located in a valley outside the city. Low wind speeds are the first of the explanatory factors. The average value of wind speed is around 1.5 m/s is nearly half of the average in Hungary (2.5-3.5 m/s). During the daytime, however, there are no major differences compared to other stations.

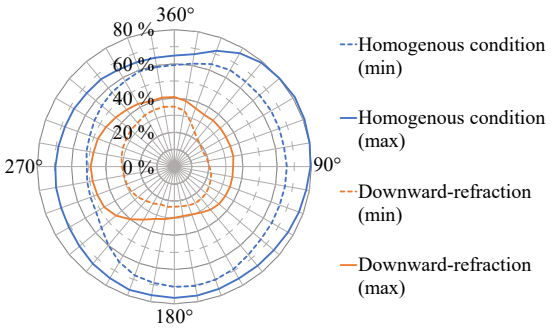

Figure 5: Minimum and maximum annual frequencies (in %) of homogeneous condition and downward-refraction cases for noise pollution for 10 years (2009-2018), based on the hourly data during daytime hours (Budapest).

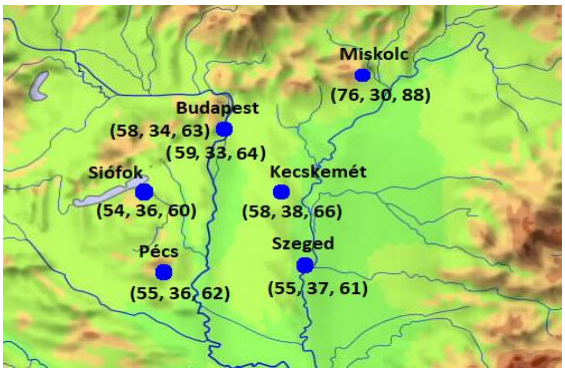

Figure 6: Relative frequencies (p_f, %) of downward-refraction cases for two 5-year periods for Budapest (2009-2013, top) and 2014-2018, bottom) and for five other Hungarian cities (2014-2018). The values in parentheses represent the nighttime, daytime, and evening hours, respectively.

Finally, the applicability of the ERA5 database in noise propagation tasks was analysed. The data of the nearest grid point to the Pestszentlőrinc (12843) station were processed. Our results for the year 2014 are shown in Table 8. Thus, we can compare the probability (p_f) data based on i) directly calculated from the measured data (SYNOP, 12843), ii) the hourly meteorological data (ERA5 MET) and iii) turbulence characteristics (u_*, T_*, L_*) from the ERA5 reanalysis dataset (ERA5 FLUX). Significant differences are found between p_f values calculated using measured and reanalysed meteorological data especially in the evening and in the nighttime, while the daytime values show a surprising similarity. The p_f data calculated from the measured values and ERA turbulence characteristics show a strong agreement at all three times of the day. Differences are below 3%.

Further analysis is required for a more detailed explanation. In any case, it can be concluded that the ERA5 database has „suitable room" for further investigation.

Table 8: Measured and calculated p_f values from the ERA5 database for the Budapest grid point based on hourly data for three time periods in 2014.

Data source	Night	Day	Evening
SYNOP	59%	33%	65%
ERA5 met	48%	35%	51%
ERA5 flux	58%	36%	68%

5. SUMMARY

A meteorological preprocessor was developed for the CNOSSOS-EU noise propagation model to separate homogeneous conditions (favourable) and downward-refraction (unfavourable) noise pollution situations for different times of the day based on the atmospheric stability, temperature and the wind speed and direction data. A virtual noise source was placed around the imaginary receptor point every 10 degrees. Our main conclusions from the investigation of a 10-year dataset for Budapest (12843) are:

- Strong up-winds ($a = -1$) and down-winds ($a = +1$) are most frequent in the main wind directions (NW, SE), while slow winds ($a = \pm 0{,}4$) are generally 30-60 degrees different, while light and crosswinds ($a = 0$) are most frequent in perpendicular to the main wind direction.
- High winds are more frequent during the day.
- The directional distribution of the up- and down-wind cases is almost a mirror image of each other.
- As expected, the most downward-refraction situations for propagation occur in the evening and at night in about 2/3 of the cases, and during the day in about 1/3 of the cases.

Analyses of data from five other Hungarian weather stations, except Miskolc, show the general features. The station at Miskolc is in a valley represented by low wind speed, which does not give

representative results. There were few variations among other stations. There is also moderate variability in the p_f probability values among years.

The ERA5 reanalysis dataset can be successfully used to build a noise propagation meteorological preprocessor. However, significant differences are found between the meteorological reanalysis data and the computations based on the ERA5 derived turbulence parameters. Using i) more stations and ii) grid cells from the ERA5 provides a sensitivity analysis of the preprocessor based on a different set of universal functions, which is also an important goal for the near future.

ACKNOWLEDGEMENTS

The authors would sincerely like to thank Viola Prohászka and Dr. Edina Balogh of the KTI Institute for Transport Sciences Non-profit Ltd. for bringing attention to the topic and their scholarly advice. They would also like to thank Peter Musyimi, who proofread and checked the grammar. This work has been supported partly by the Hungarian National Research, Development, and Innovation Centre under contract No. K-138176.

REFERENCES

[1] Guski, R., Schreckenberg, D., and Schuemer, R., 2017: "WHO Environmental Noise Guidelines for the European Region: A Systematic Review on Environmental Noise and Annoyance", *Int. J. Environ. Res. Public Health,* Vol. 14(12)*,* 1539.

[2] Deepak, J., 2016: "Noise Pollution: A Review", Int. *J Environ. Res. Pub. H.*, Vol. 4(3), pp. 72-77.

[3] Outdoor sound propagation (MSZ 15036), 2002: *Hungarian Standards Institution* (MSZT) (In Hung.)

[4] Krapf, G., and Wetzel, G., 2005: "Adaptation of national noise prediction methods to Directive 2002/49/EC Requirements on Noise Mapping", *Forum Acusticum Conference*, Budapest Hungary, pp. 995-998.

[5] Cserny, A., Tóvári, K., and Domokos, E., 2009: "The experiences of the environmental noise effect examination of industrial and service enterprises", *Acta Univ.* Sapientiae*, Agric. Environ.*, Vol. 1, pp. 151-156.

[6] Environmental noise in Europe — 2020: *EEA Report No 22/2019*. Luxembourg: Publications Office of the European Union, ISBN 978-92-9480-209-5, ISSN 1977-8449

[7] Commission Directive (EU) "2015/996 of 19 May 2015 establishing common noise assessment methods according to Directive 2002/49/EC of the European Parliament and of the Council" (Text with EEA relevance), *Official Journal of the European Union*. L, 168.

[8] Defrance, J., Salomons, E., Noordhoek, I., et al., 2007: "Outdoor Sound Propagation Reference Model Developed in the European Harmonoise Project", *Acta Acustica united with Acustica*, Vol. 93, pp. 213-227.

[9] NMPB2008, 2008: "Methodologic guide, Road noise prediction 2 - Noise propagation computation method including meteorological effects (NMPB2008)", Reference: *0957-2A.*

[10] Environmental NORD2000, 2006: *NORD2000 for road traffic noise prediction. WP4. Weather classes and statistics*. VTT Raimo Eurasto Espoo 7.4., 25 p.

[11] Hersbach, H., Bell, B., Berrisford, P., et al., 2020: "The ERA5 global reanalysis", *Q. J. R. Meteorol. Soc.*, Vol. 146(730), pp. 1999-2049.

[12] Arya, P. S., 2001: *Introduction to Micrometeorology*, 2nd Edition, Elsevier.

[13] Foken, T., 2017: *Micrometeorology*, Second Edition, and Springer Nature.

[14] Garrett S.L., 2020*: Reflection, Transmission, and Refraction. In: Understanding Acoustics*. Graduate Texts in Physics. Springer.

[15] Attenborough, K., 2014: *Sound Propagation in the Atmosphere*, in: Springer Handbook of Acoustics, 117-155.

16] Weidinger, T., Pinto, J. and Horváth, L., 2000: "Effects of uncertainties in universal functions, roughness length, and displacement height on the calculation of surface layer fluxes", *Z. Meteorol*., Vol. 9(3), 139-154.

[17] Mohan, M., and Siddiqui, T.A., 1998: "Analysis of Various Schemes for the Estimation of Atmospheric Stability Classification", *Atmospheric Environ*., Vol. 32(21), pp. 3775-3781.

[18] Holtslag, A.A.M., and Van Ulden, A.P., 1983: "A simple scheme for daytime estimates of the surface fluxes from routine weather data", *J. Appl. Meteorol. Climatol.,* Vol. 22(9), pp. 517-529.

[19] Weidinger, T., Nagy, Z., Baranka, Gy, Mészáros, R., Gyöngyösi, A.Z., 2008: "Determination of Meteorological Preprocessors for Air Quality Models in the New Hungarian Standards", *Hrvat. Meteoroloski Cas.*, Vol. 43, 6 p.

[20] Businger, J.A., Wyngaard, J.C., Izumi, Y., and Bradley, E.F., 1971: "Flux-Profile Relationships in the Atmospheric Surface Layer", *J. Atmos. Sci.*, Vol. 28(2), pp. 181-189.